NUMERICAL APPLICATION FOR THE JOHNSON-COOK MATERIALS MODEL APPLIED ON THE MODIFIED PARALLEL SHEAR ZONE OXLEY´S MACHINING MODEL FOR TI6AL-4V

Marcelo Acacio Rodrigues, marcelo.lean.engenharia@gmail.com
UniABC – Universidade do Grande ABC
Amauri Hassui, ahassui@fem.unicamp.br
Unicamp – Universidade de Campinas – Departamento de Engenharia Mecânica

Abstract. *The plastic behavior of the material has been evaluated during the machining operation with the Slip Line Field plasticity theory and the Johnson-Cook´s constitutive material´s model. The cutting force estimation has used the modified parallel shear plane zone machining model assured by P.L.B. Oxley and an ancient Slip Line solution presented by Lee and Shaffer. Several face milling operations under conventional cutting conditions onto a titanium base alloy has been observed. The feed rate, the rake angle and the cutting speed were manipulated aiming the evaluation of the residual strains under different strain rates. The specimen has been evaluated in its strained condition throughout the use of scanning electronic microscopy. Furthermore with the mathematical modeling it has been possible to conclude that the residual strain at the cross sectional surface is supportable and the strained profile can be evaluated through the use of the Slip Line Field plasticity theory. The continuum plasticity has been the main aspect to evaluate the stresses and also the strains in the workpiece and also at the chip. The materials strain hardening index is main point for a new evaluation of the P.L.B Oxley machining model, and the understanding of how the mechanical properties related with this index influence the residual plane strain and the other convergence conditions of strain during the machining are suggested in order to build up the understanding of this contribution.*

Keywords: Johnson-Cook; Oxley; Strain; Cutting forces; Continuum mechanics

1. INTRODUCTION

The machining operation can be characterized as the higher strain rate metal working operation, and after all, there is an evident separation of an amount of material. This amount removed from the bulk material is called chip. The chip formation is strictly related with the plastic condition provided by the working material and the cutting conditions.

It is important to express that the plastic conditions offered by the material are strain rate dependent because the chip formation forces equilibrium are totally related with the cutting speed and feed rate applied onto the machining process. However, if the cutting speed increases, the cutting temperature increases also. Thus, the temperature is another variable totally related with the chip formation operation.

Several plastic models were presented for metal working without chip formation, but machining process is a specific operation which a well solved model is still to be defined. There are too many applications for plastic models extracted from other metal working operation but despite the fact that there is a final separation of the working material, the metal cutting operation has a explicit difficult to be modeled. Oxley (1989) observed this difficulty and by the use of plastic models based on slip line field analysis, following Hill (1950) and Lee and Shaffer (1951), he suggested a reasonable metal cutting model which became the base for several numerical applications for understanding chip formation.

The base of the Oxley (1989) machining model is force equilibrium at the cutting interface. This interface is mapped by a slip line field, primary defined by Hencky *apud* Hill (1950) and at this region the materials are supposed to flow in a rigid plastic behavior and shear zone is parallel to the slip lines.

Since the equilibrium at the cutting interface is not fully reached, an evident unbalance of the cutting forces is observed and no convergence of the numerical model happens. The shear plan angle is the final result for this convergence. If this value agrees with the geometric condition, it is assumed that all the other metal cutting results are in equilibrium.

Oxley (1989) plastic flow consideration is based on Mises criteria. This consideration is also the base for the Lee and Shaffer (1951) cutting model. A small progress was observed onto the classical consideration of the plastic flow for ductile material, suggested by Mises as the maximum distortion energy method.

The recent years observed a growing use of the Johnson and Cook (1983) materials model. The reason for this application is the time-temperature dependent model suggested which improves the material constitutive consideration for whatever modeling to be studied.

The materials list observed by Johnson and Cook (1983) for the theory consolidation were fully expanded and nowadays is possible to get the parameters for this model for a huge amount of materials. This paper is about the alpha-beta titanium alloy Ti6Al-4V and despite the extensive use of this material onto the aeronautic industry, this data is commercially easy finding.

An experimental procedure was proceeded in other to consolidate an external influence on the calculated values based on the Oxley (1989) parallel shear zone theory with the Johnson and Cook (1983) material model.

2. BIBLIOGRAPHIC REVIEW

2.1. The Oxley parallel shear zone model

Observing the machining phenomena as an ultimate strain condition provided by the cutting tool (master) on the working material (slave), it is proposed the use of the modified parallel shear zone suggested by Oxley (1989). This model considers that the force involved in the metal cutting operation is a function of the strain rate, cutting temperature, material properties and the geometric and dynamic conditions that belong to the machining system in which the materials are about to be cut.

The modified Oxley (1989) parallel shear zone model differs from models that use the shear plane solution mainly for the assumption that the material strengths during the cutting operation. This condition is not observed with great efficiency with other machining solutions.

The basis of Oxley's model (1989) is to examine the stress distribution along the shear plane and cutting interface in terms of the shear angle, the yielding properties of the material and cutting geometry.

Oxley suggests equilibrium between the forces at the cutting interface and those at the shear plane. A fundamental hypothesis of the model is that shear plane and cutting interface are supposed to be at the direction of the maximum shear stress and maximum strain rate.

The Oxley (1989) model is based on the classic study of plasticity proposed by Hill (1950) with the use of Slip Line Fields Analysis. This plasticity model is specified for plane strain and also large deformation fields. Machining is a large deformation metal working procedure.

Figures 1 and 2 present the idealized Oxley model (1989).

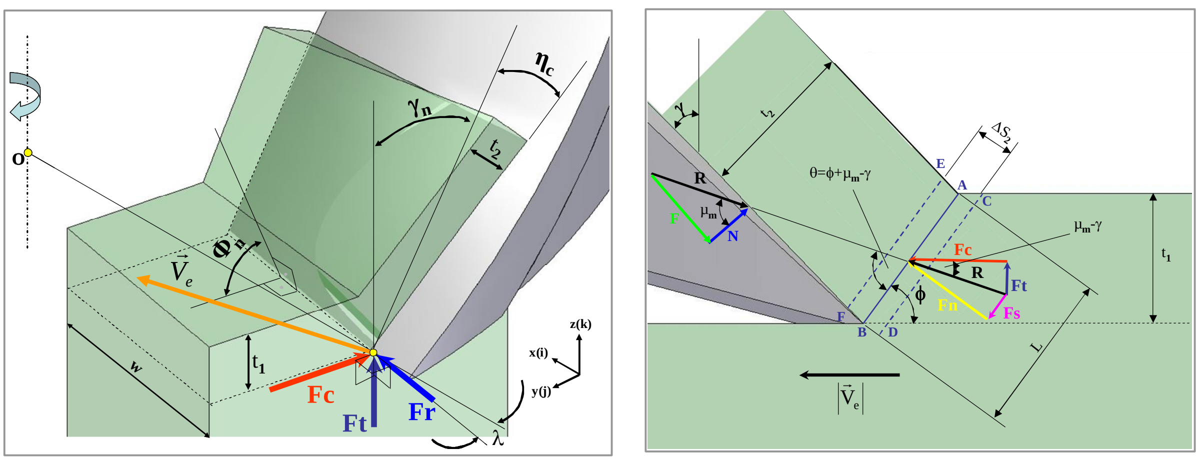

Figure 1. Idealized cutting operation and the force vectors and angles (left). Planar simplification (right)

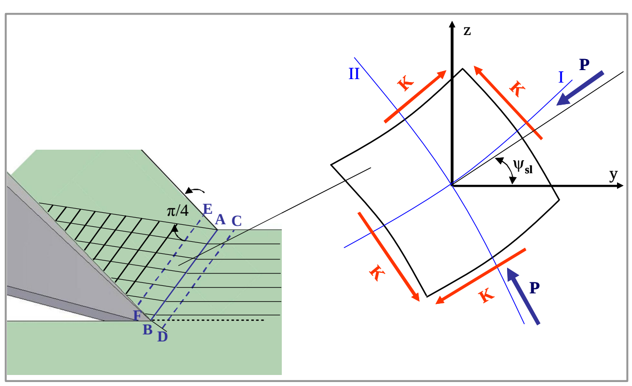

Figure 2. Shear plan zone and the slip line field detail.

The following set of equations simplifies the modified parallel shear zone Oxley´s (1989) machining method. These equations are the base for the numerical analysis of this paper. Initially, the geometric determination must be done following the equations 1 to 6, according to Zorev (1966). Equation 3 is particularly proposed by Acacio (2009).

$$\tan \eta c = \tan(\lambda) \text{ x sen } (\gamma_{\mathbf{n}}) \tag{1}$$

$$\tan \gamma_{\mathbf{n}} = \tan(\gamma) / \cos(\lambda) \tag{2}$$

$$\phi = (\phi_{\mathbf{min}} + \phi_{\mathbf{máx}})/2 \tag{3}$$

$$t_2 = \frac{t_1 \cos(\phi - \gamma)}{sen\phi} \tag{4}$$

$$\Delta s_2 = \frac{t_1}{10 \text{ x sen}(\phi)} \tag{5}$$

$$L_{AB} = \frac{t_1}{\text{sen}\,\phi} \tag{6}$$

From equations 1 to 5: ηc is the chip flow angle, $\gamma_{\mathbf{n}}$ is the orthogonal rake angle, λ is the cutting edge inclination angle, γ is the rake angle, ϕ is the shear plane convergence angle, $t_{\mathbf{1}}$ is the undeformed chip thickness, $t_{\mathbf{2}}$ is the deformed chip thickness and Δs_2 is the shear zone width variation.

After defining the geometric considerations, it is possible to define the strain conditions following the equations 7 to 13, according to Oxley (1989).

$$\gamma_{sp} = \frac{\cos(\gamma)}{\text{sen}(\phi) \text{ x } \cos(\phi - \gamma)} \cong \frac{Vs}{Vn} \tag{7}$$

$$\dot{\gamma}_{sz} = \frac{Vs}{\Delta s_2} \tag{8}$$

$$\sigma_{CD} = K_{CD}\sqrt{3} \tag{9}$$

$$\sigma_{EF} = \sigma_1 \varepsilon_{EF}{}^{n} \tag{10}$$

$$\Delta_K = K_{EF} - K_{CD} \tag{11}$$

$$\Delta_K = m \text{ x } \gamma_{EF} \tag{12}$$

$$K_{AB} = K_{CD} + \left(\frac{1}{2} m \text{ x } \gamma_{EF}\right) \tag{13}$$

From equations 7 to 13: $\gamma_{\mathbf{sp}}$ is deformation at the shear plane, Vs is the shear velocity at the shear plane, Vn is the normal velocity related to the shear velocity, $\dot{\gamma}_{sz}$ is the strain rate at the shear zone, σ_{CD} is the stress at CD plan, σ_{EF} is the stress at EF, n is the work hardening coefficient, σ_1 is the stress related with the end of the elastic region of the stress – strain diagram for the working material, ε_{EF} is the deformation at the plan EF, $K_{\mathbf{EF}}$ is the shear stress at EF plan, $K_{\mathbf{CD}}$ is the initial stress at the end of the elastic region, ΔK is shear stress variation occurred during the chip formation, *m* is a geometrical constant and $K_{\mathbf{AB}}$ is the shear stress at the main shear plan AB.

After defining the strain and strain rate conditions, it is possible to define the slip line strain conditions following the equations 14 to 28, according to Oxley (1989).

$$\tan\theta = 1 + 2 \text{ x} \left(\frac{\pi}{4} - \phi\right) - \frac{\Delta K}{2K_{AB}} \frac{L_{AB}}{\Delta s_2} \tag{14}$$

$$\theta = \phi + \mu_{\mathbf{m}} - \gamma \tag{15}$$

$$C = \frac{1}{n} \frac{\Delta K}{2K_{AB}} \frac{L_{AB}}{\Delta s_2} \tag{16}$$

$$\tan\theta = 1 + 2 \text{ x} \left(\frac{\pi}{4} - \phi\right) - \frac{\Delta K}{2K_{AB}} \frac{L_{AB}}{\Delta s_2} \tag{17}$$

$$\dot{\gamma}_{AB} = \frac{C \text{ x } V_S}{L_{AB}} \tag{18}$$

$$Fs = K_{AB} \text{ x } L_{AB} \text{ x } w \tag{19}$$

$$Fn = \left(\frac{P_A + P_B}{2}\right) \text{x } L_{AB} \text{ x } w \tag{20}$$

$$L_{int} = \frac{t_1 \text{ x } sen\theta}{\cos\mu_m \text{ x } sen\phi}\left\{1 + \frac{Cn}{3 \text{ x}\left[1 + 2\left(\frac{\pi}{4} - \phi\right) - Cn\right]}\right\} \tag{21}$$

$$\dot{\gamma}_{int} = \frac{V}{\delta t_2} \tag{22}$$

$$F = R \text{ x } sen\,(\mu_{\mathbf{m}}) \tag{23}$$

$$N = R \text{ x } \cos\,(\mu_{\mathbf{m}}) \tag{24}$$

$$\tau_{int} = \frac{F}{L_{int} \text{ x } w} \tag{25}$$

$$\sigma_{int} = \frac{N}{L_{int} \text{ x } w} \tag{26}$$

$$R = \frac{K_{AB} \text{ x } t_1 \text{ x } w}{sen\phi \text{ x } \cos\theta} \tag{27}$$

$$K_{chip} = \frac{\sigma_1}{\sqrt{3}} \tag{28}$$

From equations 14 to 28: θ auxiliary angle, μm is the mean friction angle, $\dot{\gamma}_{AB}$ strain rate at the main plane AB, Fs is the shear force at the shear plane, w is the cutting width, $P_{\mathbf{A}}$ is the hydrostatic pressure at the point A, $P_{\mathbf{B}}$ is the hydrostatic pressure at the point B, Lint is the cutting interface length, F is the friction force at the interface, N is the normal force at the interface, $\tau_{\mathbf{int}}$ is the shear stress at the interface, $\sigma_{\mathbf{int}}$ the normal stress at the interface, R is the resultant cutting force and $K_{\mathbf{chip}}$ is the shear stress at the chip.

The final convergence for the Oxley model occurs when a selected shear plane angle provides a residual or null result for the convergence proposed by equation 29.

$$K_{\mathbf{chip}} \rightarrow \tau_{int} \tag{29}$$

2.2. The Johnson and Cook constitutive materials model

The machining process itself must be considered as a coupled deformation process where no change in the cutting speed is able to keep the temperature at the same level. This means that every perturbation at the cutting parameters will result dynamically at the cutting temperature and strain rate. By this reason a thermoviscoplastic materials model fits with less assumption the machining process.

Oxley (1989) considered a simple plastic model to fit his conclusions of convergences. Oxley began a plasticity implementation process and the recent researches mutually agree with the use of Johnson-Cook constitutive materials model.

Johnson and Cook (1983) proposed the equation 30 as the solution for thermoviscoplastic problems in which the strain rate and the deformation temperature can’t be neglected.

$$\sigma = \left[A + B \text{ x } (\varepsilon^{pl})^n\right] \text{x} \left[1 + C \text{ x } \ln\left(\frac{\dot{\varepsilon}^{pl}}{\dot{\varepsilon}_0}\right)\right] \text{x} \left[1 - \left(\frac{T - T_{ref}}{T_{fusão} - T_{ref}}\right)^m\right] \tag{30}$$

The machining process itself must be considered as a coupled deformation process where no change in the cutting speed is able to keep the temperature at the same level. This means that every perturbation at the cutting parameters will change the temperature level.

From equation 30: σ is the dynamic flow stress, A is the initial yielding stress, B is the resistance coefficient, ε^{pl} is the total plastic strain, n is the work-hardening index, C is the strain sensitivity, $\dot{\varepsilon}^{pl}$ is the total plastic strain rate, $\dot{\varepsilon}_0$ is the reference plastic strain, T is the temperature, T_{ref} is the reference temperature, $T_{fusão}$ is the melting temperature and m is the thermal softening.

Su (2006) and other researchers concluded a set of equations in order to actualize those presented by Oxley (1989). This new set of equations has the purpose of introducing the dynamic behavior at the deformation phenomena which takes place during the machining operation. Equations 31 to 35 are responsible for this actualization.

$$\sigma_{\text{AB}} = \left[A + B \text{ x } (\varepsilon_{\text{AB}})^n\right] \text{x} \left[1 + C \text{ x } \ln\left(\frac{\dot{\varepsilon}_{\text{AB}}}{\dot{\varepsilon}_0}\right)\right] \text{x} \left[1 - \left(\frac{T_{AB} - T_{ref}}{T_{fusão} - T_{ref}}\right)^m\right] \tag{31}$$

$$\sigma_{\text{EF}} = \left[A + B \text{ x } (\varepsilon_{\text{EF}})^n\right] \text{x} \left[1 + C \text{ x } \ln\left(\frac{\dot{\varepsilon}_{\text{EF}}}{\dot{\varepsilon}_{AB}}\right)\right] \text{x} \left[1 - \left(\frac{T_{\text{int}} - T_{ref}}{T_{fusão} - T_{ref}}\right)^m\right] \tag{32}$$

$$\sigma_{\text{chip}} = \left[A + B \text{ x } (\varepsilon_{\text{chip}})^n\right] \text{x} \left[1 + C \text{ x } \ln\left(\frac{\dot{\varepsilon}_{\text{chip}}}{\dot{\varepsilon}_{SZ}}\right)\right] \text{x} \left[1 - \left(\frac{T - T_{ref}}{T_{fusão} - T_{ref}}\right)^m\right] \tag{33}$$

$$\tan\theta = 1 + 2 \text{ x } \left(\frac{\pi}{4} - \phi\right) - \text{Cn} \tag{34}$$

$$\text{Cn} = \text{C}_{\text{Oxley}} \text{ x n x } \left(\frac{\text{B x } \varepsilon_{\text{AB}}^{\text{n}}}{\text{A} + \text{B x } \varepsilon_{\text{AB}}^{\text{n}}}\right) \tag{35}$$

From equations 31 to 35: $\sigma_{\mathbf{AB}}$ is the dynamic flow stress at plane AB, $\dot{\varepsilon}_{AB}$ is the total plastic strain rate at the plane AB and $T_{\mathbf{AB}}$ is the temperature at the plane AB. The index EF and chip indicates the other plane position at the cutting model (see Figure 1).

Acacio (2009) proposed a correction of equations 30 to 34 based on the flowing concept. This idea is supported by the reason that the present state of flowing is a continuity of the previous state. Many researchers preceded these equations without this correction, but the results obtained in this investigation are enough to consolidate this correction. The continuity idea is idealized in Figure 3.

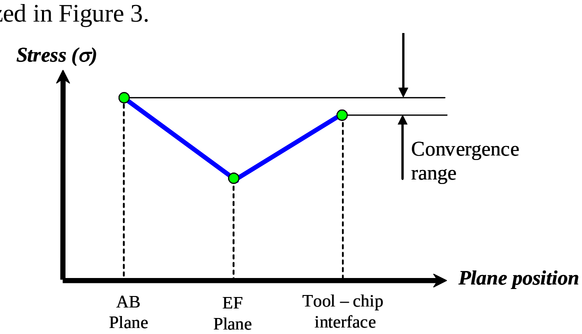

Figure 3. Idealized continuity of the plastic flow along the plane position during machining.

2.3. The alpha+beta Titaniun alloy Ti6Al-4V

The titanium base alloy Ti6Al-4V is characterized by its high mechanical resistance associated with low density, low thermal conductivity, good thermal stability under high temperatures, good fatigue resistance, corrosion resistance, biocompatibility and cryogenic profile.

The Ti6Al-4V has a HC matrix (alpha phase). The secondary phase is CCC. Reinforced intermetalic phases and chemical stabilizers are also found at this microstructure.

The chemical elements addition will increase or decrease the temperature range and also the medium temperature where the titanium alloy will present an allotropic transformation from at the HC (α) to the CCC (β) microstructure.

In most of the titanium alloys, the equilibrium field for the phases α and β are separated by a secondary phase called α + β (alpha plus beta). At this secondary phase, under specific temperature and chemical balance, a martensitic transformation takes place from beta to alpha martensitic. This transformation is a consequence for the fast cooling thermal treatment that the alloy at the phase beta is submitted, resulting in a martensitic microstructure.

As an example of the chemical stabilizers addition, the molybdenum addition at the Ti6Al-4V provides a delay at the separation between α and β. The aluminum addition suggests a reinforced microestructure once the aluminum and the titanium have good chemical affinity and the aluminum is not spread within the microestructure interstitially.

The Figure 4 presents the Ti6Al-4V microstructure and its phases as cited above.

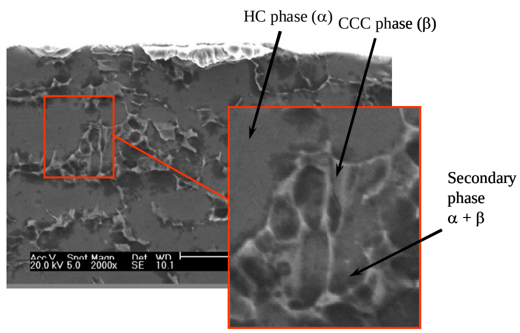

Figure 4. Ti6Al-4V microstructure and its phases.

3. EXPERIMENTAL PROCEDURE

3.1. Materials and equipments

A face milling operation has been executed under several cutting conditions. The details for this operation are listed below.

Machine: Deckel Maho 63V vertical milling center

Cutting tool: 10mm solid carbide end mill. The details for the cutting tools are presented at table 1.

Table 1. Cutting tools specification.

Designation	*Din Specification*	*N° of Tooth*	*γ axial*	*γ radial*	*Substrate*	*Cover layer*
A	DIN 6527	3	45º	0°	WC+C K20	TiAlN
B	DIN 6527	4	30º	0°	WC+C K20	TiAlN

Material Sample: Ti6Al-4V blocks at the dimension of 37 x 35 x33 (mm). The mechanical and thermal properties of the sample applied are presented at table 2. Johnson-Cook parameters are presented at table 3

Table 2. Mechanical and thermal properties of the samples.

Young Modulus (GPa)	113,8
Yielding limit (MPa)	880
Rupture limit (MPa)	950
Elongation %	14%
Hardness (HRc)	27,3
Specific heat J/ (g° C)	0,5263
Thermal condutivity W/ (m x K)	6,7
Melting point (°C)	1604~1660
Density (g/cm^3)	4,43

Table 3. Johnson-Cook parameters, after Lesuer (1999)

Material	*A*	*B*	*C*	n	m
Ti-6Al-4V (21)	862	331	0,012	0,34	0,8
	(MPa)	(MPa)	( )	( )	( )

Measurement: Olympus optical microscope Bx60M with 20, 50 100, 200 e 500X magnification. Philips electronic microscope.

3.2. Experimental routine

Figure 5 presents the samples before and after the face milling operation.

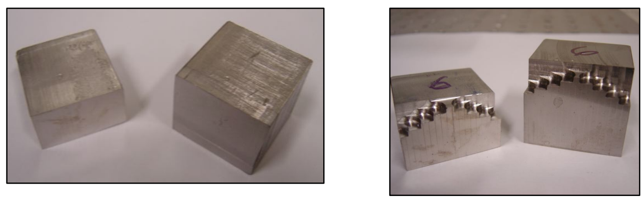

Figure 5. Sample before (left) and after (right) the face milling operation.

The cutting depth applied was 2 mm for every experiment. Cutting fluid was also applied. The cutting speed were 37,5 , 45, 52,5 and 60 m/min. The feed per teeth were 0,08 , 0,096 and 0,112 mm/teeth. Down milling and up milling were conducted with the two types of cutting tools listed at Table 1. The combination of all these conditions totalizes 48 experiments.

All the samples were observed at the optical and the microscope. The results were measured and the deformation lines were modeled with the cutting forces provided by the mathematical procedure cited at 2.1 and 2.2.

4. RESULTS AND DISCUSSION

4.1. The aplication of the modified parallel shear plane machining theory with the Johnsono-Cook constitutive materials model

The Table 4 presents the input data for γ equal 30 and λ equals zero degree and the Tables 5 and 6 presents the results for two conditions selected among the experiments cited at 3.2

Table 4. Input data for γ equal 30 and λ equals zero (radial and axial rake angles).

Iten	Symbol	Values				Unit
Cutting speed	Vc	37,5	45	52,5	60	m/min
Cutting width	W	0,06897	0,06897	0,06897	0,06897	mm
Minimum shear plane angle	Φ_{min}	24,45	22,74	21,65	20,88	(°)
Maximum shear plane angle	$\Phi_{máx}$	40,1	40,06	40,065	40	(°)
Work Hardening index	N	0,34	0,34	0,34	0,34	( )
Yielding stress	σ_{CD}	862,000	862,000	862,000	862,000	MPa
Deformation at the yielding point	ε_{CD}	0,0076	0,0076	0,0076	0,0076	( )
Young modulus	E	113800,000	113800,000	113800,000	113800,000	MPa
Plastic deformation efficiency factor at AB	Nf	0,950	0,950	0,950	0,950	( )
Temperature variation at the cutting interface permission factor	ψt	0,950	0,950	0,950	0,950	( )
$\sigma 1$ from simple plasticity relation	σ_1	856,903	856,903	856,903	856,903	MPa
Initial temperature at AB	T_0	20,000	20,000	20,000	20,000	°C
Constant A	A	862,000	862,000	862,000	862,000	MPa
Constant B	B	331,000	331,000	331,000	331,000	MPa
Constant C	C	0,012	0,012	0,012	0,012	( )
Constant m	M	0,800	0,800	0,800	0,800	( )
Interface temperature for the Johnson-Cook model from simple plasticity model	*T*	232,834	241,489	248,461	254,242	°C

The Table 4 presented a sample of the values that were applied for each simulated condition with a specific combination of rake angles, cutting speed and feed per teeth. Twelve tables like Table 4 were produced in order to feed the model with all the simulated condition. Table 5 presents the calculated results applying the equations presented in 2.1.

Table 5. Calculated results following the equations 1 to 35.

Iten	Symbol	Values				Unit
Chip flow angle (Zorev)	ηc	0,000	0,000	0,000	0,000	(°)
Chip flow angle (Kronnemberg)	ηc	0,000	0,000	0,000	0,000	(°)
Normal rake angle	γn	30,000	30,000	30,000	30,000	(°)
Shear plane convergence angle	Φ	32,275	31,400	30,858	30,440	(°)
Deformed chip thickness	t_2	3,742	3,838	3,899	3,947	Mm
Shear zone width variation	Δs_2	0,375	0,384	0,390	0,395	mm
Normal velocity	Vn	20,024	23,445	26,927	30,398	m/min
Shear velocity	Vs	32,502	38,983	45,471	51,963	m/min
Rigid chip velocity	V	20,040	23,452	26,931	30,399	m/min
Deformation at the shear plane	γ_{sp}	1,623	1,663	1,689	1,709	( )
Strain rate at the shear zone	$\dot{\gamma}_{sz}$	1446,275	1692,534	1943,542	2193,862	1/s
Strain rate at EF plane	$\dot{\varepsilon}_{EF}$	835,007	977,185	1122,105	1266,627	1/s
Shear strain at EF plane	γ_{EF}	1,623	1,663	1,689	1,709	( )
Deformation at EF plane	ε_{EF}	0,937	0,960	0,975	0,987	( )
EF plane Stress - Johnson-Cook constitutive model	σ_{EF}	959,640	953,681	948,658	944,475	MPa
Stress at EF plane	K_{EF}	554,049	550,608	547,708	545,293	( )
Deformation along the AB plane	ε_{AB}	0,469	0,480	0,487	0,493	( )
Stress along the shear plane	K_{AB}	582,296	580,232	578,247	576,473	MPa
Stress at AB Plane - Johnson-Cook constitutive model	σ_{AB}	1008,566	1004,992	1001,553	998,481	MPa
AB plane length	L_{AB}	3,745	3,839	3,899	3,948	Mm
Auxiliar angle	θ	54,153	54,738	55,091	55,359	(°)
Mean friction angle	μm	51,878	53,338	54,234	54,919	(°)
Oxley´s C Constant (actualized)	Cn	0,060	0,060	0,061	0,061	( )
Strain rate along AB plane	$\dot{\gamma}_{AB}$	8,682	10,225	11,790	13,351	1/s
Strain rate at AB plane	$\dot{\varepsilon}_{AB}$	903,845	1111,078	1316,495	1523,057	1/s
Shear strain at AB plane	γab	0,811	0,831	0,844	0,855	1/s
Hydrostatic pressure at A	p_A	840,944	855,686	863,708	869,460	MPa
Hydrostatic pressure at B	p_B	817,173	831,849	839,856	845,605	MPa
Shear force along the AB plane	Fs	150,420	153,620	155,513	156,954	N
Normal force along the AB plane	Fn	428,329	446,783	458,154	466,955	N
Shear zone temperature variation	ΔTsz	231,126	247,393	260,209	271,178	°C
Temperature along the AB plane	T_{AB}	228,013	242,654	254,189	264,060	°C
Interface temperature	T_{int}	285,438	303,553	316,998	327,996	°C
Maximun temperature increase at the interface	$\Delta\theta m$	36,118	38,062	38,724	38,756	°C
Mean temperature increase	$\Delta\theta c$	49,205	52,404	54,409	55,972	°C
Contact interface length	L_{int} (h)	4,989	5,324	5,548	5,730	mm
Chip width variaton at the rectangular plastic zone	δ	1,091	1,171	1,249	1,322	mm
Deformation at the chip	ε_{CHIP}	1,643	1,644	1,633	1,621	( )
Strain rate at the chip	$\dot{\varepsilon}_{CHIP}$	88,381	96,321	103,709	110,600	1/s
Shear stress at the tool-chip interface	τint	566,912	561,951	557,549	553,598	MPa
Normal stress at the tool-chip interface	σint	444,863	418,293	401,616	388,796	MPa
Johnson-Cook stress at the chip	$\sigma chip$	981,848	973,349	965,713	959,220	MPa
Actualized stress at the chip	K_{chip}	566,870	561,963	557,555	553,806	MPa
Resultant force	R	247,960	257,239	262,943	267,358	N
Cutting force	Fc	230,101	236,193	239,772	242,468	N
Orthogonal force	Ft	92,399	101,904	107,928	112,649	N
Radial force	Fr	0,000	0,000	0,000	0,000	N
Friction force at the interface	F	195,070	206,349	213,355	218,791	N
Normal force at the interface	N	153,074	153,597	153,685	153,659	N
Convergence	$K_{chip} - t_{int}$	-0,042	0,012	0,006	0,207	( )
Feed direction force	Fy	216,943	222,687	226,061	228,603	N
Ortogonal to feed force direction force	Fx	76,696	78,726	79,919	80,818	N
Ortogonal feed force	Fz	92,399	101,904	107,928	112,649	N

All the geometric values obtained at Table 5 are based on Zorev (1989). The main values can be understood following the equations 1 to 6. The other results are cited by Oxley (1989), referring the same Zorev (1966). Thermal values are obtained from Bothrooyd *apud* Oxley (1989), Su (2006) and Acacio (2009).

Figure 6 presents the strained profile of the workpiece submitted to the cutting conditions showed above. Six samples were produced equally to that one presented below. All the strained measurements were performed with electronic microscopy.

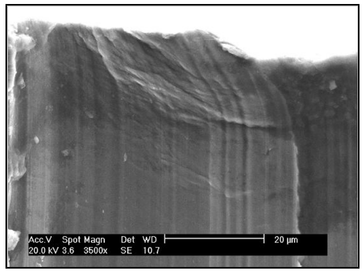

Figure 6. Cross section of the machined sample. Cutting speed (v_c) is 60m/min, feed per teeth (f_z) is 0,08 mm/teeth and axial rake angle is 45°.

Figure 7 presents the graphic profile of the results presented at Table 4.

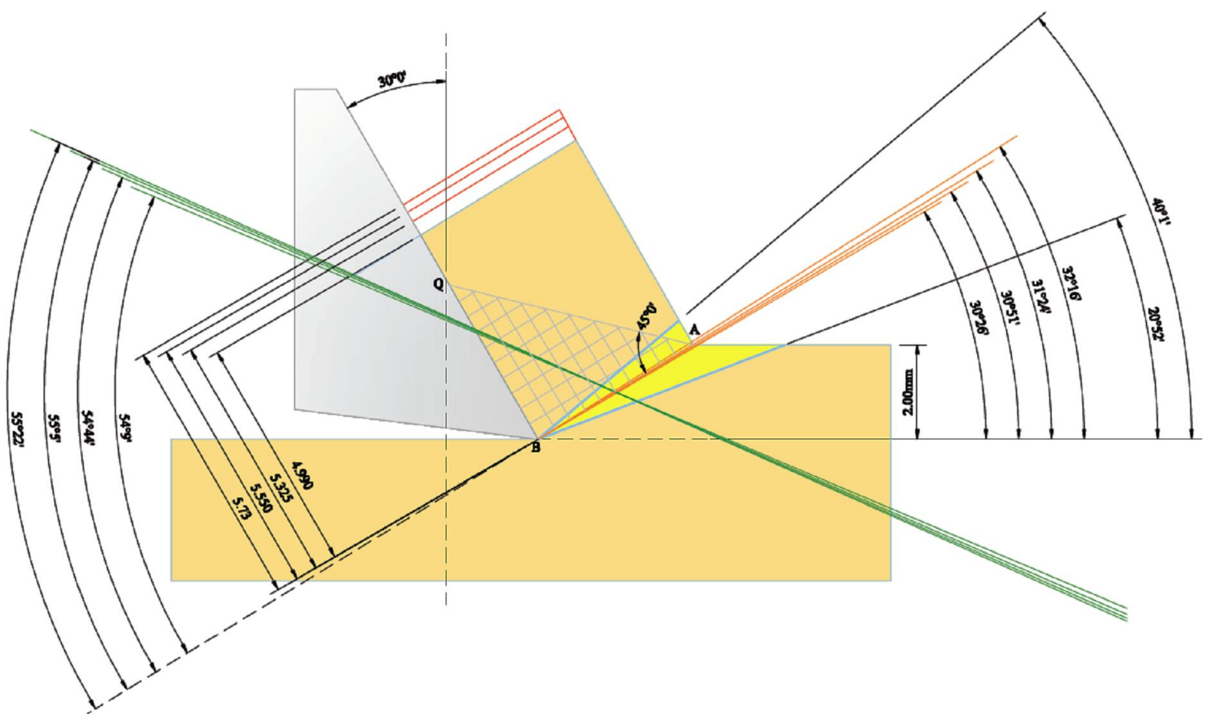

Figure 7. Application of the results calculated with the suggested model. The green lines present the direction of the convergence when the cutting speed is manipulated.

It was observed from Table 4 that the convergence is in agreement with the expected results. This condition is plainly satisfied when the convergence number rounds zero. Figure 6 is also an evidence that there is a strained profile after the machining process and the correlation showed by Acacio (2009) is supportable and converges with the Oxley (1989) machining model. Figure 7 has been extracted from a group of graphics and it synthesizes the idea of force equilibrium at the cutting interface and all the force profile based in this model supports the strained profile of the piece.

One important point that was observed during the execution of the trials was the material machinability sensitivity to deformation. This aspect is related with the strain hardening index. Titanium presents the value of 0,34 for this index and no adjust has been done at the equations for reaching the convergence. This condition satisfies not only the Oxley (1989) condition but also the correlation between cutting forces and force equilibrium proposed by Oxley (1989) and the strained profile measurement, proposed by Acacio (2009).

The manipulation of the strain hardening index conducted to a conflicting numerical condition for the Oxley (1989) where an ancient machining theory proposed by Lee and Schaffer (1951) is about to solve without the use of constants, as we can see at the Oxley (1989) model.

5. CONCLUSIONS

After the observations of the results above, it is possible to conclude that:

- The Oxley machining model (1989) can be actualized by the use of the Johnson-Cook (1983) materials constitutive model;
- The slip line field plasticity model, proposed by Hill (1950) is in accordance with the strained profile observed after the milling process, measured and suggested by Acacio (2009);
- The titanium strain hardening index can be considered as an average value and it represents an important influence in the convergence;
- The angles suggested for the equilibrium among all the cutting conditions satisfies not only graphically but also dynamically the machining model;
- The strained profile measurement and its interpretation are a small part of the analyses but it conducts to the conclusion that unavoidable damage occurs at the workpiece after the machining process.

6. REFERENCES

ACACIO, M.R. 2009. "Uma contribuição para o estudo das deformações residuais proporcionadas pelo processo de fresamento". PHD Thesis, São Paulo State University, 220 p.

HILL, R., 1950."The mathematical theory of PLASTICITY". Oxford, Clarendon Press, 356p.

JOHNSON, G.R.; COOK, W. H.,1983 "A constitutive model and data for metals subjected to large strains, high strain rates and high temperatures". Proc. 7th Int. Symp. on Ballistics, 541-547. Hague, The Netherlands

LEE, E.H.; SHAFFER, B.W., 1951."The Theory of Plasticity Applied to a Problem of Machining". Transactions of ASME, vol. 73

LESUER, R.; KAY, G. J.; LEBLANC, M. M.,1999. "Modeling Large-Strain, High-Rate Deformation in Metals – Third Biennial Tri-Laboratory Engineering Conference Modeling and Simulation" - Pleasanton, CA / 3-5 – 1999

OXLEY, P.L.B., 1989."Mechanics of machining – An analytical approach to assessing machinability". Ellis Horwood Limited

SU, J-C., 2006."Residual stress modeling in machining processes". PHD Thesis, Georgia Institute of Technology, 180p.

ZOREV, N.N., 1966 "Metal Cutting Mechanics". Pergamon Press, 525p

7. RESPONSIBILITY NOTICE

The authors are the only responsible for the printed material included in this paper.